

# Dielectric properties of Zn-Ti substituted BaFe<sub>12</sub>O<sub>19</sub>

<sup>1</sup>Vaishali Soman,<sup>2</sup>V. M. Nanoti,<sup>3</sup>Vijay Soman

<sup>1</sup>Assistant Professor,<sup>2</sup>Professor,<sup>3</sup>Associate Professor

<sup>1</sup>Department of Applied Physics,

Priyadarshini Indira Gandhi College of Engineering, Nagpur, India

<sup>3</sup>S.M. Mohota Science College, Nagpur

**Abstract :** The Fe<sup>3+</sup> ions in BaFe<sub>12</sub>O<sub>19</sub>, were partially substituted by Zn<sup>2+</sup> and Ti<sup>4+</sup> ions. This paper reports the study of the dielectric properties of the compounds BaFe<sub>12-2x</sub>Zn<sub>x</sub>Ti<sub>x</sub>O<sub>19</sub> ( $x = 1, 1.5, 2$ ) synthesized using the solid state diffusion method. The plots of variation between real ( $Z'$ ) and imaginary ( $Z''$ ) parts of impedance show the decrease of grain resistance with increase in temperature as well as concentration of substitution ( $x$ ). In these plots the shift in the peak positions of the semi-circles with the change in temperature suggests the variation of relaxation time which indicates thermally activated conduction mechanism. The variation of  $M'$  and  $M''$  (real and imaginary parts of dielectric modulus respectively) with frequency has also been carried out in the present study. The value of  $M'$  increases with increase in frequency at various temperatures.

**Key words:** Magnetoplumbite, grain boundary, Dielectric properties, Impedance, Dielectric modulus, Cole-Cole plots.

## I. INTRODUCTION

Barium hexaferrite (BaFe<sub>12</sub>O<sub>19</sub>) or BaM is well studied hexagonal M-type ferrimagnetic material due to its number of applications in high density magnetic recording, electrical and electronic devices, transformers, etc.<sup>[1-6]</sup> Since these hexaferrites also have a potential application as high frequency absorbing materials many researchers have studied the effect of substitution of Fe<sup>3+</sup> ions with other divalent - tetravalent metal ion combinations such as Zn<sup>2+</sup>-Sn<sup>4+</sup>, Co<sup>2+</sup>-Sn<sup>4+</sup>, Ni<sup>2+</sup>-Zr<sup>4+</sup>, Co<sup>2+</sup>-Ti<sup>4+</sup>, Mn<sup>2+</sup>-Ti<sup>4+</sup>, etc.<sup>[6]</sup>

The structural, magnetic, electrical and the dielectric properties of the substituted hexaferrites strongly depend on the electronic configuration of the substituted cations, their site preferences, concentration of the substituents as well as the methods of synthesis. Many authors investigated these properties for Zn<sup>2+</sup>-Ti<sup>4+</sup> substituted BaM ferrite. Haijun et al.<sup>[6]</sup> synthesized Ba(ZnTi)<sub>x</sub>Fe<sub>12-2x</sub>O<sub>19</sub> ( $0.2 \leq x \leq 1.0$ ) by sol-gel method and observed dispersion in complex permeability in the study of their dielectric properties in the microwave frequency range (100 MHz – 6.0 GHz). The work was further carried out by Dube et al.<sup>[7]</sup> for low concentration of substitution of Zn<sup>4+</sup>-Ti<sup>2+</sup> in BaFe<sub>12-2x</sub>Zn<sub>x</sub>Ti<sub>x</sub>O<sub>19</sub> ( $0.2 \leq x \leq 0.6$ ) and for two frequency ranges 8-13GHz and 1kHz-1MHz. Wartewig et al.<sup>[8]</sup> extensively studied only the magnetic properties of these samples at higher concentrations of Zn<sub>x</sub><sup>4+</sup>-Ti<sub>x</sub><sup>2+</sup> ( $0 \leq x \leq 2.0$ ) by means of magnetization (SQUID), neutron diffraction and Mössbauer measurements.

The dielectric properties of these materials arise due to intra-grain, inter-grain and other electrode effects. The motion of charges could take place by charge displacement, dipole orientation, space charge formation, etc. In order to understand the electrical properties, the grain, grain boundary and the electrode contributions must be separated out.<sup>[9]</sup> Complex impedance analysis is a powerful tool for separating out these contributions. In the present study, therefore, the complex impedance spectra of the sample BaFe<sub>12-2x</sub>Zn<sub>x</sub>Ti<sub>x</sub>O<sub>19</sub> ( $x = 1, 1.5, 2$ ) has been analyzed and explained using the Cole-Cole expression as a function of frequency and temperature.

## 2. Experimental

Polycrystalline hexaferrites with composition BaFe<sub>12-2x</sub>Zn<sub>x</sub>Ti<sub>x</sub>O<sub>19</sub> were synthesized by the conventional ceramic technique using high purity Fe<sub>2</sub>O<sub>3</sub> (Sigma – Aldrich), ZnO, BaO and TiO<sub>2</sub> (all Merck). The structural and morphological properties of these samples were investigated with XRD (X-ray diffraction) and SEM (Scanning electron microscopy) respectively and described elsewhere<sup>[10]</sup> along with the detailed procedure of synthesis.

The dielectric and impedance measurements, as a function of frequency ( $f$ ) in the range 100 Hz to 10 MHz, temperature ( $T$ ) and range 30 °C to 345 °C and composition ( $x$ ) ( $x = 1, 1.5, 2$ ) were carried out by Alpha-AN impedance analyzer from Novocontrol (Germany).

## 3. Results and Discussion:

### 3.1. Structural Properties:

To XRD and SEM studies of all these samples were carried out and the results were published elsewhere<sup>[10]</sup>. These results show that all the samples are single phase magnetoplumbite with hexagonal structure and the SEM study shows well formed grains separated by prominent grain boundaries.

### 3.2. Dielectric Properties:

The dielectric properties are often represented in terms of complex impedance ( $Z$ ), complex permittivity ( $\epsilon$ ) and the electrical modulus ( $M$ ) which offer wide scope for analysis and usually it is necessary to study at least two properties so as to extract maximum amount of information. [11] In the present study the Cole-Cole plots, variation of impedance and dielectric modulus with respect to frequency and temperature has been carried out.

As stated earlier, the complex impedance analysis is a useful investigation technique as the impedance of the grains is separated from other sources of impedance, namely grain boundaries and electrode effect. It also gives the information about resistive ( $Z'$ ) and the reactive ( $Z''$ ) components of impedance of the material. Figure 1(a) shows the variation of  $Z'$  with frequency, for the sample  $x = 1$ , at some temperatures. The samples with  $x = 1.5, 2$  also show a similar nature for the variation of  $Z'$  with frequency as shown in Figure 1(b-c) respectively. At lower frequencies the magnitude of  $Z'$  is of  $10^5$ - $10^6 \Omega$  order and shows a gradual decrease with the increase in frequency. This observation is true at low temperatures, particularly up to  $97^\circ\text{C}$ . Beyond this temperature, the magnitude of  $Z'$  is of  $10^2$ - $10^3 \Omega$  order and remains constant with a plateau till almost up to  $10^5$  to  $10^6$  Hz, which refers to the dc conduction and hence constant impedance is observed. This decrease of  $Z'$  with increase in frequency is attributed to the space charge polarization. The samples under study are in the form of well formed grains which are conducting in nature. The grains are separated by well formed grain boundaries which act as insulators. When external field is applied, the electrons start hopping between  $\text{Fe}^{2+}$  and  $\text{Fe}^{3+}$  ions which is responsible for the conductivity in the samples. At lower frequencies of the field these electrons cannot cross the barrier of the grain boundary and accumulate near the boundary. This increases space charge polarization and thus impedance shows high values at lower frequencies [9-12]. As the frequency increases, the electrons gain sufficient energy to cross the barrier of grain boundary which increases the conductivity and hence impedance shows smaller values. Further, the decrease of  $Z'$  with the increase in temperature can be related to the charge ordering phenomenon with temperature and these results are in good agreement with those earlier reported in similar ferrites. [13]

Figure 2 (a) shows variation of  $Z''$  with frequency for temperature range  $30^\circ\text{C}$ - $97^\circ\text{C}$  and Figure 2 (b) shows this variation for temperature range  $198^\circ\text{C}$  -  $345^\circ\text{C}$ . It can be seen in Figure 2(a) that beyond a certain frequency, all the curves coalesce and  $Z''$  becomes constant and independent of frequency and temperature. However, in Figure 2(b),  $Z''$  is found to be independent of temperature and frequency up to  $10^3$  Hz for the same sample, but beyond this frequency, dispersion is observed. These curves show  $Z''$  to be maximum ( $Z''_{\text{max}}$ ) at a certain frequency and with the increase in temperature, the peak is observed to shift towards higher frequency 'which indicates multiple relaxation process in the materials and the decrease of  $Z''$  and the reduction of space charge polarization'. [14] The decrease of  $Z''_{\text{max}}$  with the increase in temperature is attributed to decrease of the reactance of the sample.

The curves between  $Z''$  and  $Z'$  are known as Cole-Cole plots which can give semicircles depending on the electrical properties of the materials. The total complex impedance of the system at an applied frequency is expressed as a sum of the real and imaginary components of the material.

$$Z^*(\omega) = Z'(\omega) + iZ''(\omega) \quad (1)$$

According to Koop's model the ferrite material can be assumed to be made up of parallel conducting plates separated by resistive plates which correspond to the grain and grain boundaries respectively. The semicircle at low frequency represents resistance of grain boundary ( $R_{gb}$ ) and the one at higher frequency corresponds to resistance of the grain ( $R_g$ ) or bulk property. These resistances  $R_g, R_{gb}$  are obtained from the circular arc intercepts on  $Z'$  axis. The capacitance of the grain and that of the grain boundary are represented as  $C_g$  and  $C_{gb}$  and the maximum height of the semicircle gives capacitances  $C_g$  and  $C_{gb}$  which can be calculated from the relations:

$$C_g = \frac{1}{R_g \omega_g} \quad (2)$$

and

$$C_{gb} = \frac{1}{R_{gb} \omega_{gb}} \quad (3)$$

where,  $\omega_g$  and  $\omega_{gb}$  correspond to the frequencies at the peak of the semicircle of grain and grain boundary respectively. Further, each point on the complex impedance plot or Cole-Cole plot ( $Z''$  versus  $Z'$ ) represents a particular frequency. Figures 3-5 show the complex impedance plots for all the ferrites  $x = 1, 1.5$  and  $2$  respectively at different temperatures. 'In a complex impedance plane, grain, grain boundary and grain-electrode effects appear as semicircles where the lower frequency arc corresponds to the grain boundaries, while the high frequency arc represents the grain'. [14] It is clearly seen from these plots that the semi-circular arcs merge together and terminate on the higher frequency side of  $Z'$  axis. Further, as no second semi-circle is obtained, it can be concluded that the grain boundary resistance is negligibly small as compared to the grain resistance. The various impedance parameters calculated using these equations for all samples at room temperature have been summarized in Tables 1-3. With the rise in temperature, it is observed that the peak of the semi-circle is shifting to higher frequency which suggests that the 'conduction mechanism is a thermally activated one'. [11] Further, the semi-circular arc corresponding to grain gets gradually suppressed with increase in temperature. With the increase in concentration of  $\text{Zn}^{2+}$  and  $\text{Ti}^{4+}$ , height and area of semicircles decrease. Thus the resistance decreases with the increase in temperature as well as concentration of substituted cations.

The frequency dependence of real ( $M'$ ) and imaginary ( $M''$ ) parts of the electrical modulus at various temperatures for the samples  $x = 1, 1.5, 2$  is as shown in Figures 6 and 7 respectively.

It can be seen from Figures 6 (a-c) that qualitatively the nature of all the curves is almost similar where a gradual increase in  $M'$  with the increase in  $f$  is observed. The curves shift towards the high frequency region with the increase in temperature. Except for the ferrite  $x = 1$ , these curves do not coalesce and dispersion is observed for the complete range of frequency.

The variation of  $M''$  with frequency for the ferrites  $x = 1, 1.5, 2$  is as shown in Figures 7(a-c). A broad peak in the spectrum undergoes a systematic shift in its position towards high frequency with the increase in temperature for  $x = 1.5$  and  $2$ . The peak also

gets broadened with the increase in temperature which indicates 'temperature dependent relaxation process with different mean time constant of the relaxation process suggesting a non-Debye type of relaxation in the material'.<sup>[13]</sup>

### Conclusions

In the parent compound  $\text{BaFe}_{12}\text{O}_{19}$ ,  $\text{Zn}^{2+}$  and  $\text{Ti}^{4+}$  ions were partially substituted using the solid state diffusion method to get the compounds  $\text{BaFe}_{12-2x}\text{Zn}_x\text{Ti}_x\text{O}_{19}$  ( $x = 1, 1.5, 2$ ). It was observed that the grain resistance decreases with increase in temperature as well as concentration of substitution ( $x$ ). In the Cole-Cole plots the shift in the peak positions of the semi-circles with the change in temperature suggests the variation of relaxation time which indicates thermally activated conduction mechanism. The value of  $M'$  increases with increase in frequency at various temperatures.

### Acknowledgements

One of the authors VVS is thankful to UGC-DAE-BARC- Mumbai, STIC-Kochi, IIT- Kanpur, HBCSE-Mumbai (all these laboratories are in India) for technical help.

### References:

1. Fortes S. S., Duque J. G. S., Macedo M. A., *Physica B***2006**, 384, 88.
2. Zhang X., Duan Y., Guan H., Liu S., Wen B., *J. Magn. Magn. Mater.* **2007**, 311, 507.
3. Haq A., Anis-ur-Rehman M., *Physica B***2012**, 407, 822.
4. Soman V. V., Nanoti V. M., Kulkarni D. K., *Ceramics Int.* **2013**, 39 5713.
5. Almeida R. M., Paraguassu W., Pires D. S., Correa R. R., de A. Paschoal C.W., *Ceram. Int.***35** (2009) 2443.
6. Haijun Z., Zhichao L., Chengliang M., Xi Y., Liangying Z., Mingzhong W. *Materials Sci. And Engg.* **B96** (2002) 289-295.
7. Dube C. L. , Kashyap S. C., Pandya D. K., Dube D. C., *Phys. Status Solidi A***206** (11) (2009) 2627.
8. Wartewig P., Krause M. K., Esquinazi P., Rosler S., Sonntag R., *J. Magn. Magn. Mater.* **192** (1999) 83.
9. Prasad N V, Prasad G, Bhimasankaram T, Suryanarayana S V, Kumar G S, *Bull. Mater. Sci.* **24** (2001) 487.
10. Soman V. V., Nanoti V. M., Kulkarni D. K., Soman V., *Phys. Procedia***54** (2014) 30-37.
11. Singh N., Agarwal A, Sanghi S, Khasa S., *J. Magn. Magn. Mater.* **324** (2012) 2506.
12. Singh N., Agarwal A, Sanghi S, *Current Appl Phys.* **11** (2011) 783.
13. Verma K, Sharma S, *Phys. Status Solidi***249** (2012) 209.
14. Ramesh B., Ramesh S., Vijaya Kumar R., LakshmipathiRao M, *J Alloys Comps***513** (2012) 289-293.



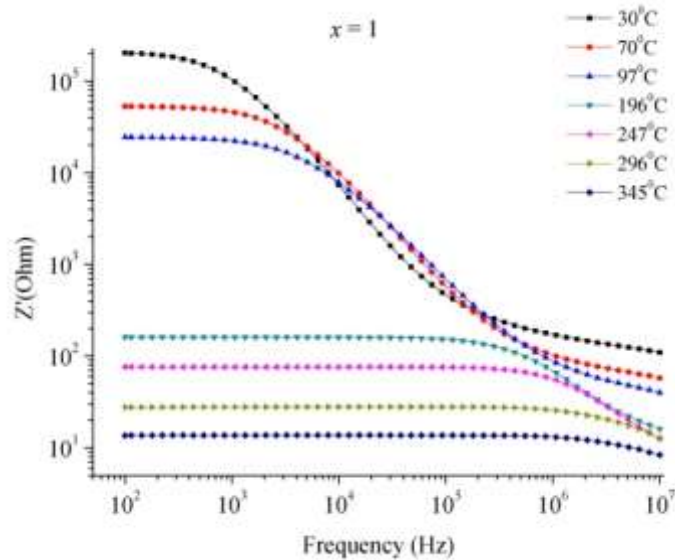


Figure 1 (a) Z'vs frequencyfor  $x=1$

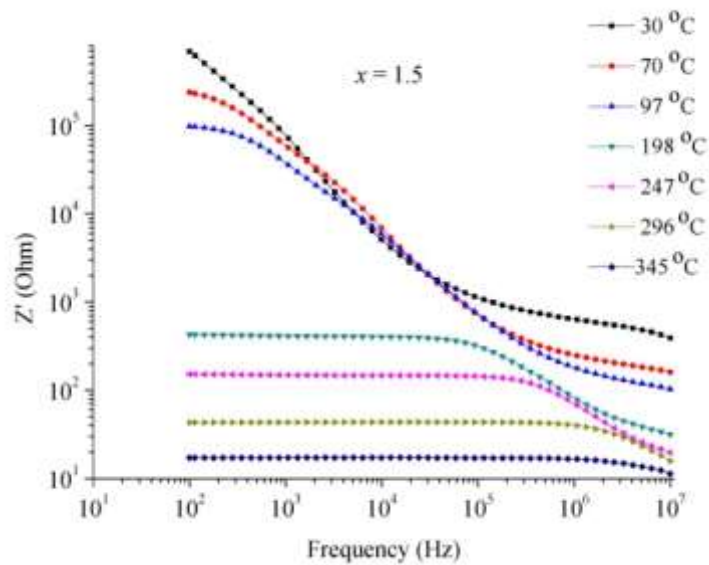


Figure 1 (b) Z'vs frequency for  $x=1.5$

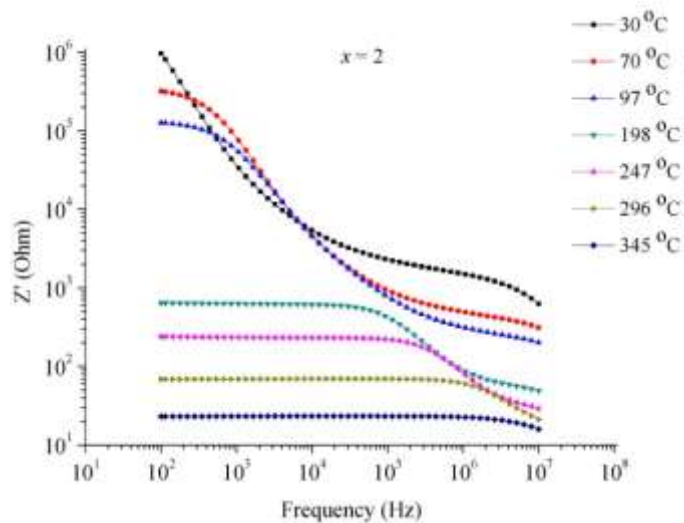


Figure 1 (c) Z'vs frequencyfor  $x= 2$

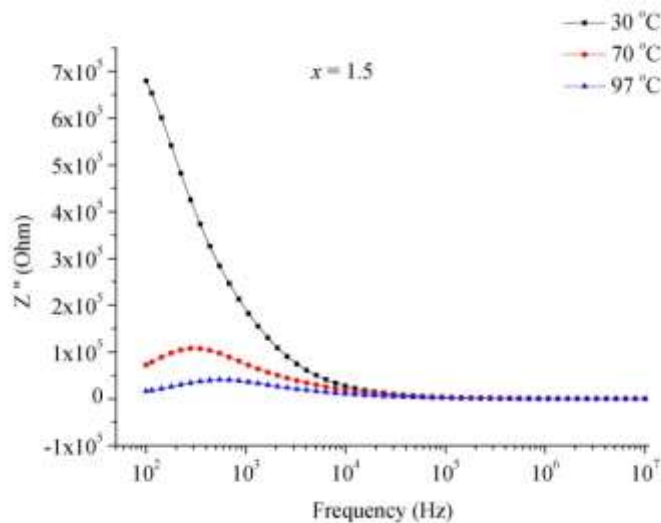


Figure 2 (a)  $Z''$  vs frequency at low Temperature

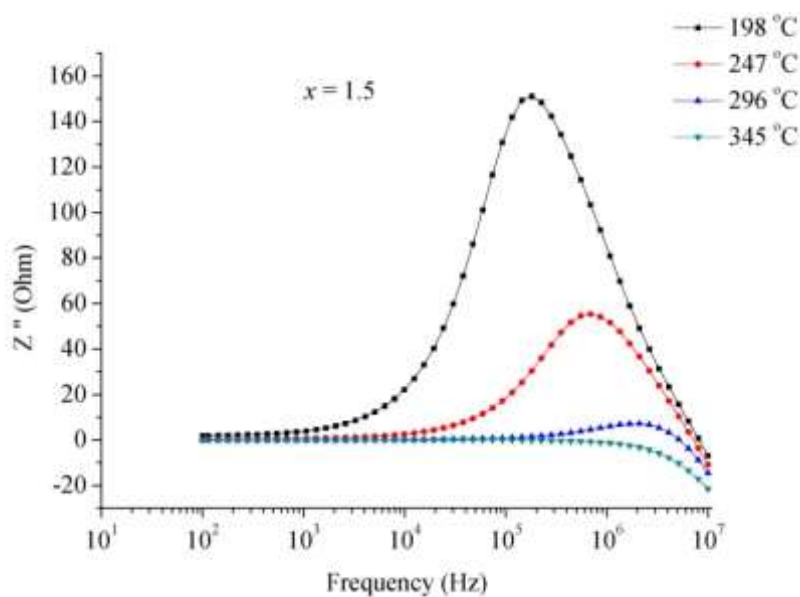


Figure 2 (b)  $Z''$  vs frequency at higher Temperature

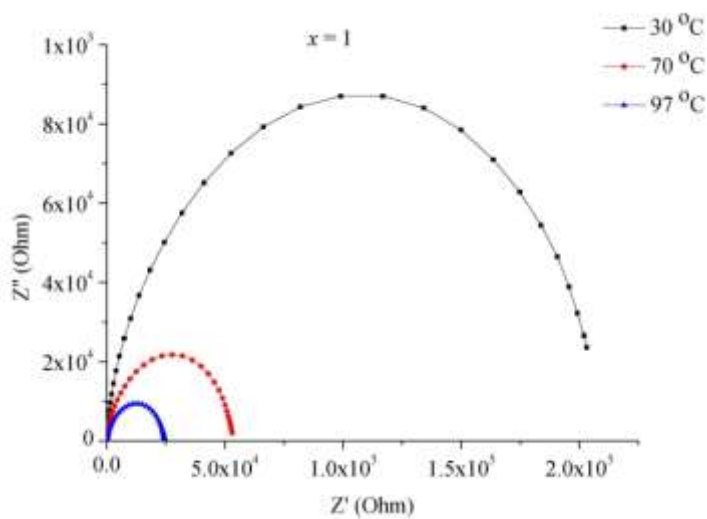


Figure 3  $Z'$  vs  $Z''$  for  $x=1$

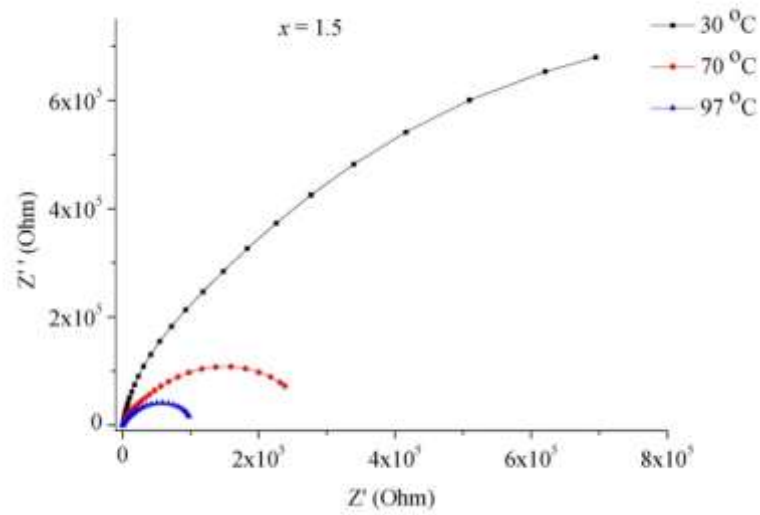


Figure4  $Z'$  vs  $Z''$  for  $x=1.5$

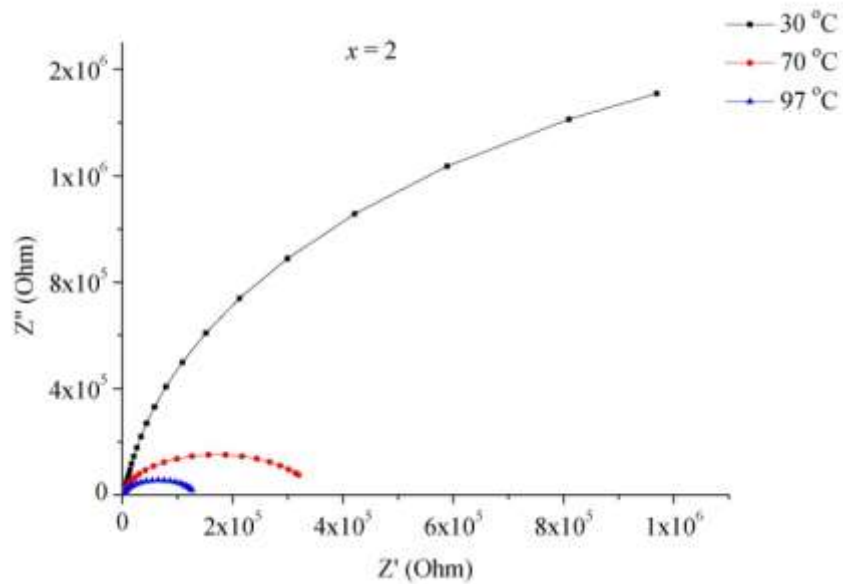


Figure5  $Z'$  vs  $Z''$  for  $x= 2$

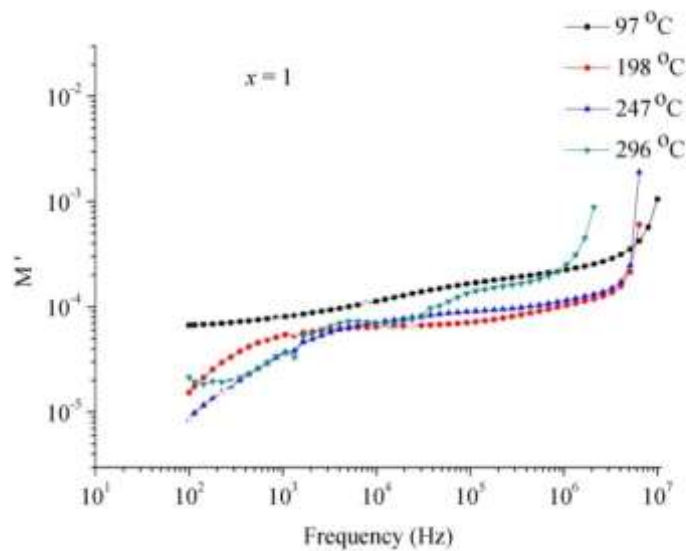


Figure 6 (a)  $M'$  vs frequency for  $x = 1$

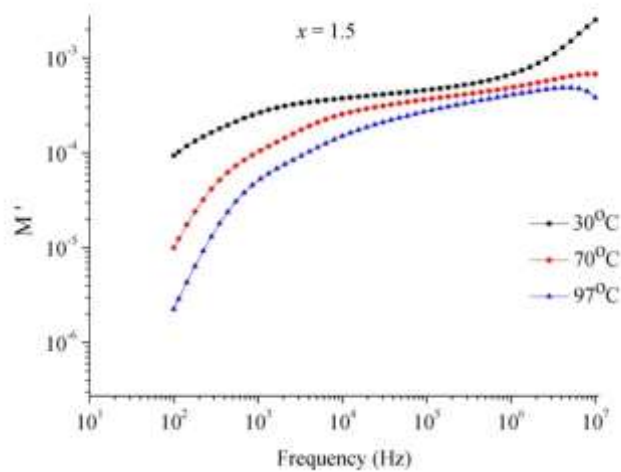


Figure 6 (b)  $M'$  vs frequency for  $x = 1.5$

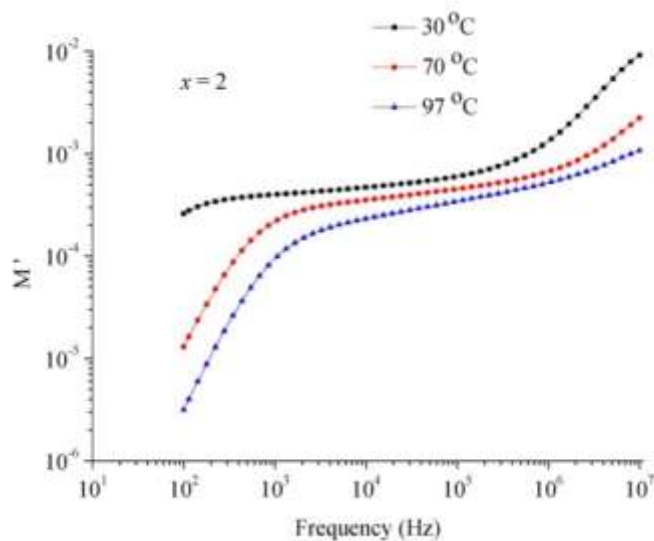


Figure 6 (c)  $M'$  vs frequency for  $x = 2$

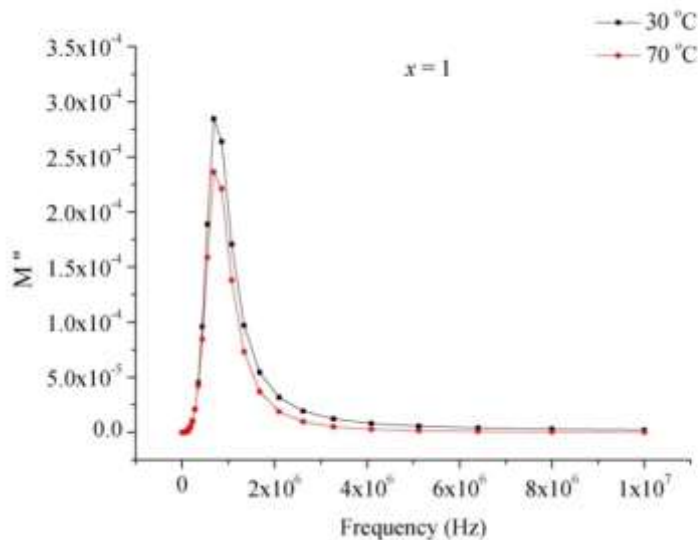


Figure 7 (a)  $M''$  vs frequency for  $x = 1$

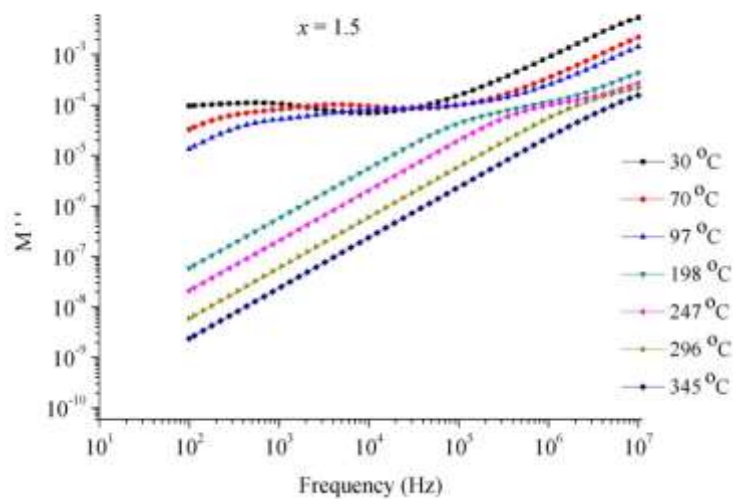


Figure 7 (b)  $M''$  vs frequency for  $x = 1.5$

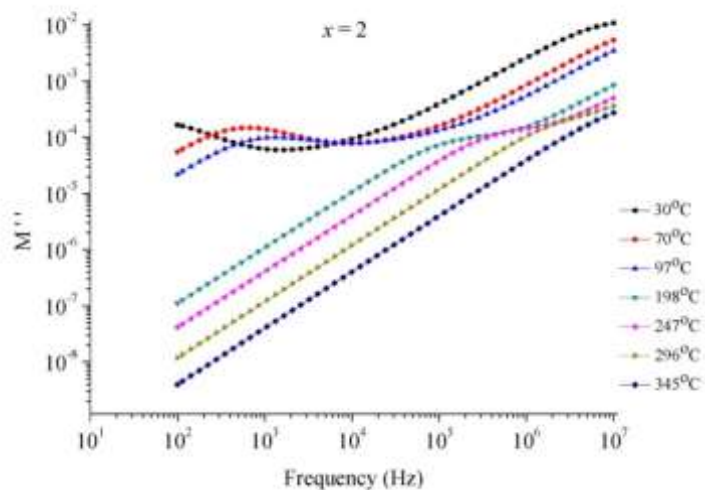


Figure 7 (c)  $M''$  vs frequency for  $x = 2$

**Table 1**Impedance parameters for  $\text{BaFe}_{12-2x}\text{Zn}_x\text{Ti}_x\text{O}_{19}$  ( $x = 1$ ) at various temperatures.

$T$ (°C)	$R_g$ ( $\Omega$ )	$f_g$ (Hz)	$C_g$ (nF)
30	$2.11 \times 10^5$	$1.063 \times 10^3$	0.709
70	$5.4 \times 10^4$	$2.596 \times 10^3$	1.135
97	$2.5 \times 10^4$	$5.070 \times 10^3$	1.256
198	$1.42 \times 10^2$	$6.871 \times 10^5$	1.628
247	59.12	$1.34 \times 10^6$	2.010

**Table 2**Impedance parameters for  $\text{BaFe}_{12-2x}\text{Zn}_x\text{Ti}_x\text{O}_{19}$  ( $x = 1.5$ ) at various temperatures.

$T$ (°C)	$R_g$ ( $\Omega$ )	$f_g$ (Hz)	$C_g$ (nF)
70	$2.97 \times 10^5$	$2.78 \times 10^2$	1.92
97	$1.05 \times 10^5$	$5.44 \times 10^2$	2.78
198	$3.93 \times 10^2$	$1.8 \times 10^5$	2.24
247	$1.29 \times 10^2$	$6.87 \times 10^5$	1.78

**Table 3**Impedance parameters for  $\text{BaFe}_{12-2x}\text{Zn}_x\text{Ti}_x\text{O}_{19}$  ( $x = 2$ ) at various temperatures.

$T$ (°C)	$R_g$ ( $\Omega$ )	$f_g$ (Hz)	$C_g$ (nF)
70	$3.48 \times 10^5$	$5.44 \times 10^2$	$8.41 \times 10^{-2}$
97	$1.27 \times 10^5$	$8.50 \times 10^2$	1.47
198	$5.90 \times 10^2$	$1.44 \times 10^5$	1.82
247	$2.02 \times 10^2$	$4.39 \times 10^5$	1.79
296	44.17	$2.09 \times 10^6$	1.72